

**NANO EXPRESS**

**Open Access**

# Electronic structures and optical properties for Ag-N-codoped ZnO nanotubes

Xian-Yang Feng, Chang-Wen Zhang, Xi-Jin Xu and Pei-Ji Wang<sup>\*</sup>

## Abstract

The structural and electronic/optical properties of pure and Ag-N-codoped (8,0) ZnO nanotubes have been studied using first-principles calculations in the framework of the local spin density approximation. The configurations for Zn atoms replaced by Ag atoms are p-type semiconductor materials, and the bandgap increases when N atoms are doped into ZnO nanotube configurations. The optical studies based on dielectric function and reflectivity indicate that new transition peaks in the visible light range are observed, which can be ascribed to the Ag and N doping. Furthermore, there is a red shift observed with the increase of N concentration.

**Keywords:** Ag-N codoped; ZnO nanotube; Electronic structure; Optical property

## Background

Since the discovery of single-walled carbon nanotubes (SWCNTs) in the early 1990s [1], the research on tubular nanostructures has attracted increasing interest because their unique structures can provide some unique properties, such as high Young's modulus, high thermal conductivity, and high aspect ratio structure. Besides SWCNTs, many other tubular nanostructures such as boron nitride nanotubes, gallium nitride (GaN) nanotubes, and zinc oxide (ZnO) nanotubes have been intensively investigated in recent years. Density functional theory (DFT) calculations have shown that the single-walled GaN, AlN, and InN nanotubes are all metastable, and they are semiconductors with either a direct bandgap (zigzag tubes) or an indirect bandgap (armchair tubes) [2-5].

Recently, Shen et al. found that ZnO single-walled nanotube (SWNT) is more/less stable than its nanowire or nanobelt if the diameter is smaller/bigger than that of (24,0) ZnO SWNT [6]. Hence, the small-diameter (8,0) ZnO SWNT is expected to be more stable. Additionally, Zhou et al. also studied the size- and surface-dependent stability of (8,0) ZnO nanotube, and found that the (8,0) ZnO nanotube had a good surface texture [7].

To get p-type doped ZnO, group V, group IA, and group IB elements have been used as dopants [8-13]. Different doping elements are favorable in O-poor/rich conditions to realize p-type doped ZnO, and the doping will easily produce oxygen vacancy defects. For example, N doping is only favorable in O-poor conditions but will easily produce oxygen vacancy defects. For element Ag, it has smaller diameter and larger ionization energy than group IA elements, and its doping process is favorable in O-rich conditions, which can suppress the defects in ZnO; thus, element Ag is a better candidate for p-type ZnO doping.

Codoping ZnO with transition metal/nonmetal ions is an effective way to modify its electronic/optical properties [14,15]. In this paper, the structure and formation energies of Ag-N-codoped ZnO nanotubes were firstly calculated using DFT and followed by the calculations on the electronic and optical properties with the optimized structures.

## Methods

Multiwalled and single-walled ZnO nanotubes with similar structures to CNTs can be successfully realized by cutting the atoms inside and outside of ZnO crystalline supercell along the *c* direction. Single-walled ZnO nanotubes can be regarded as the thinnest walled ZnO

\* Correspondence: ss\_wangpj@ujn.edu.cn  
School of Physics and Technology, University of Jinan, Jinan 250022, People's Republic of China

nanotubes whose structures are similar to CNTs. In our case, the zigzag (8,0) ZnO nanotube containing 64 atoms is selected as a prototype, as shown in Figure 1. Six other configurations based on this structure are considered for the study of the properties of Ag-N-codoped ZnO nanotubes. The first model is obtained by replacing one Zn atom with an Ag atom (Ag atom at 1 site, named as  $\text{Ag}_1$ ). For the configurations with one and two N atoms replacing two O atoms, the N atoms can be at 2 and 3, 4 sites, which are named as  $\text{Ag}_1\text{N}_2$  and  $\text{Ag}_1\text{N}_{3,4}$ , respectively. The  $\text{Ag}_1\text{N}_5$  and  $\text{Ag}_1\text{N}_6$  configurations are the ones with Ag replacing Zn at 1 site and N replacing O at 5 and 6 sites.

The first-principles full-potential linearized augmented plane wave method based on the generalized gradient approximation [16] is used for the exchange-correlation potential within the framework of DFT to perform the computations, as implemented in the WIEN2K simulation package. Special  $k$  points were generated with the  $1 \times 1 \times 4$  grid based on Monkhorst-Pack scheme. Good convergence was obtained with these parameters. The total energy was converged to be  $1.0 \times 10^{-4}$  eV/atom in the optimized structure.

## Results and discussion

### Geometry structures and formation energies

Figure 1 shows the top-view and side-view models of the optimized structures for zigzag single-walled (8,0) ZnO nanotubes. The single-walled ZnO nanotubes are obtained by folding a single-layered graphitic sheet from the polar (0001) sheet of wurtzite bulk structure. Another study showed that the ZnO nanotubes are more stable than ZnO nanowires for small diameters (the number of atoms is smaller than 38 for one unit cell) [6]. Hence, the (8,0) ZnO nanotubes (with 32 atoms in one unit cell) constructed in this paper are reasonable. The formation energies of Ag-N-codoped (8,0) ZnO

SWNT were calculated to evaluate their stability. The formation energy can be expressed as

$$E_f = E(\text{Ag}, \text{N-ZnO}) - E(\text{ZnO}) + \mu(\text{Zn})/\mu(\text{O}) - \mu(\text{Ag})/\mu(\text{N})$$

In this equation,  $E(\text{Ag}, \text{N-ZnO})$  and  $E(\text{ZnO})$  are the total energies of ZnO SWNTs with and without the impurity, respectively, and  $\mu$  is the chemical potentials of Zn, O, Ag, and N, which depend on the growth conditions. The formation energies are listed in Table 1. The formation energy of Ag-doped ZnO nanotubes is apparently smaller than Ag-doped ZnO nanowires [17], which indicates that Ag-doped nanotubes is more easily achieved than nanowires. For the configurations with N atoms replacing O atoms, the formation energy increases with the increase of N concentration, indicating that low N concentration is more stable. For the configuration with the same N concentration, the  $\text{Ag}_1\text{N}_2$  configuration is more stable than  $\text{Ag}_1\text{N}_5$  and  $\text{Ag}_1\text{N}_6$  configurations. The formation energies of  $\text{Ag}_1\text{N}_2$ ,  $\text{Ag}_1\text{N}_5$ , and  $\text{Ag}_1\text{N}_6$  are smaller than  $\text{Ag}_1\text{N}_{2,3,4}$  and  $\text{Ag}_1\text{N}_{3,4}$  configurations, which indicates single N atom doping will induce more stable structures than that of more N atoms doped. The Ag-doped (8,0) ZnO nanotube is distorted compared with the undoped one because the Ag-O bond lengths are longer than the Zn-O bond lengths. For the  $\text{Ag}_1\text{N}_2$ ,  $\text{Ag}_1\text{N}_{3,4}$ , and  $\text{Ag}_1\text{N}_{2,3,4}$  configurations, there are bonds between Ag and N atoms. The average bond lengths in these configurations and the bond lengths of Zn atoms and N atoms are displayed in Table 1.

### Electronic properties

As shown in Figure 2, the further calculation of band structure for bulk wurtzite ZnO shows a direct bandgap of 0.81 eV, which is in good agreement with the previous calculation [18], but is smaller than the experimental value. In Figure 2, the valence band maximum (VBM) of the bulk ZnO is predominantly contributed by O  $2p$  character. The conduction band minimum (CBM) basically originates from the Zn  $4s$  states with small O  $2p$  states. That is to say, the electronic transition from O  $2p$  states to Zn  $4s$  states is responsible for the optical

**Table 1 Bandgap ( $E_{\text{gap}}$ ), Zn-N bond lengths ( $R_{\text{Zn-N}}$ ), and formation energies ( $E_f$ ) of Ag-N-codoped ZnO nanotubes**

|                                     | $E_{\text{gap}}$ (eV) | $R_{\text{Ag-N}}$ (Å) | $R_{\text{Zn-N}}$ (Å) | $R_{\text{Ag-O}}$ (Å) | $E_f$ (eV) |
|-------------------------------------|-----------------------|-----------------------|-----------------------|-----------------------|------------|
| (8,0) $\text{Ag}_1$                 | 1.17                  | -                     | -                     | 1.868                 | 0.410      |
| (8,0) $\text{Ag}_1\text{N}_2$       | 1.10                  | 1.853                 | 1.838                 | 1.883                 | 0.523      |
| (8,0) $\text{Ag}_1\text{N}_{3,4}$   | 1.20                  | 1.860                 | 1.836                 | 1.893                 | 0.626      |
| (8,0) $\text{Ag}_1\text{N}_{2,3,4}$ | 1.25                  | 1.879                 | 1.833                 | -                     | 0.719      |
| (8,0) $\text{Ag}_1\text{N}_5$       | 1.15                  | -                     | 1.842                 | 1.870                 | 0.570      |
| (8,0) $\text{Ag}_1\text{N}_6$       | 1.17                  | -                     | 1.846                 | 1.869                 | 0.572      |

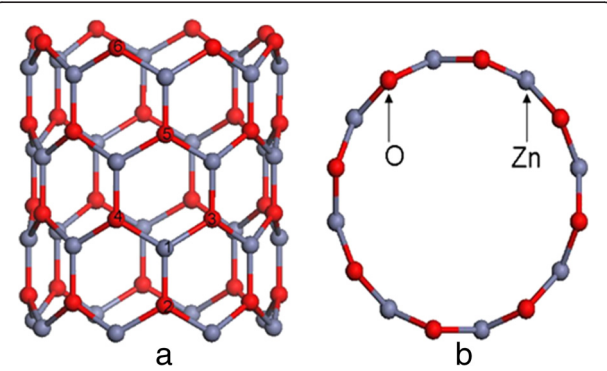


**Figure 1 (8,0) ZnO nanotube.** (a) Ag atom doped at 1 site and N atoms which can be doped at 2, 3, 4, 5, and 6 sites. (b) Top view of (8,0) ZnO nanotube. Red and gray balls represent O and Zn atoms, respectively.

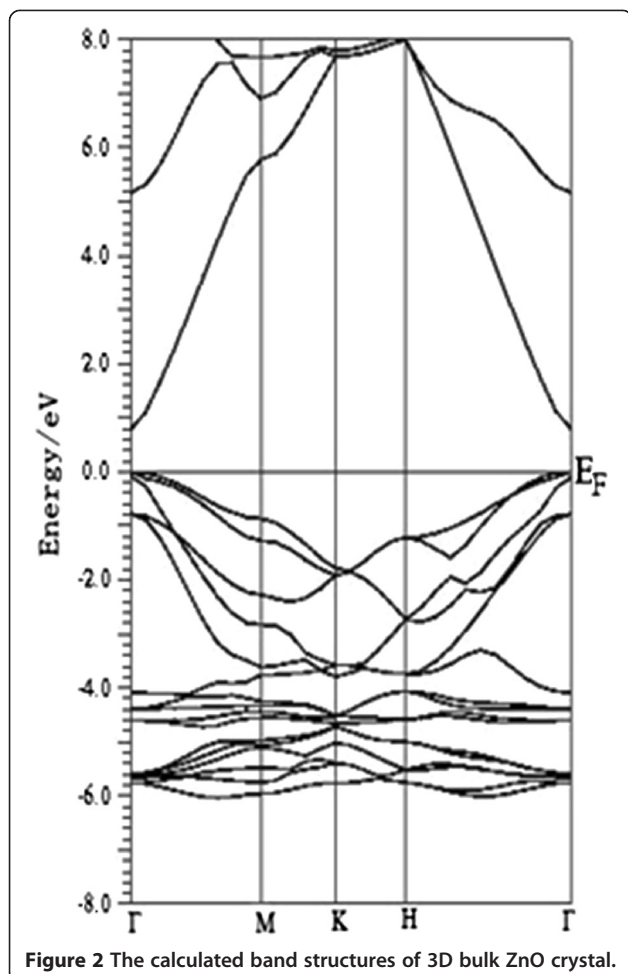


Figure 2 The calculated band structures of 3D bulk ZnO crystal.

absorption onset of pure ZnO. For the pure (8,0) ZnO nanotube, the bandgap is 1.0 eV, close to other calculated value of 1.17 eV. The bandgap of ZnO nanotube is larger than the bulk material (0.81 eV) due to the quantum confinement effect. For Ag-doped ZnO nanotube, the bandgap increases to 1.17 eV (shown in Figure 3b), and two impurity levels appear and are located below the Fermi level, which show a donor character. The calculated density of states (DOS) and project density of states (PDOS) in Figure 4a and part (a') of Figure 4b show that the two impurity levels originate from the Ag 3d states. For N-doped ZnO nanotube (configurations  $\text{Ag}_1\text{N}_2$ ,  $\text{Ag}_1\text{N}_{3,4}$ , and  $\text{Ag}_1\text{N}_{2,3,4}$ ), the bandgaps increase with the N concentrations (1.10, 1.20, and 1.25 eV, respectively) increasing. Some levels pass through the Fermi level, indicating that N impurity acts as an acceptor doping in ZnO nanotube. In  $\text{Ag}_1\text{N}_{2,3,4}$  system, it follows Figure 3e that the host valence band (VB) is surpassed and two gap states are introduced above the VB. The lowest defect level is occupied and locates at about 0.19 eV above the host VBM. Another gap state is occupied and locates at 0.22 eV above the Fermi level. However, the lowest acceptor

level in  $\text{Ag}_1\text{N}_{3,4}$  is occupied and is located at 0.04 eV around the Fermi level. All these results illustrate that  $\text{Ag}_1\text{N}_{3,4}$  demonstrates the better p-type behavior than the  $\text{Ag}_1\text{N}_{2,3,4}$  system. For the  $\text{Ag}_1\text{N}_5$  and  $\text{Ag}_1\text{N}_6$  system, the bandgaps are 1.15 and 1.17 eV, which are different to the  $\text{Ag}_1\text{N}_2$  system (1.17 eV), indicating that the bandgap has nothing with the distance of Ag atom and N atom. Before investigating the Ag doping effect on the ZnO nanotubes' optical properties, we calculated the density of states (DOS) of Ag-N-codoped (8,0) ZnO nanotubes as shown in Figure 4, which indicates that Ag-doped ZnO nanotube shows typical characters of p-type semiconductor. Figure 4a,b shows that the states located at the Fermi level are dominated by Ag 4d states and N 2p states, demonstrating the occurrence of the N 2p to Ag 4d hybridization. As discussed above, more impurity states will be introduced in the band structure with the increase of N dopant concentration. From Figure 4 (c'), we find that the hybridization between Ag atom dopant and its neighboring host atoms results in the splitting of the energy levels near the Fermi level, which shifts to the majority spin states downward and minority spin states upward to lower the total energy of the system.

#### Optical properties

As discussed, the optical properties of pure and Ag-N-codoped (8,0) ZnO nanotubes are based on the dielectric function, absorption coefficient, and reflectivity. In the linear response range, the solid macroscopic optical response function can usually be described by the frequency-dependent dielectric function  $\varepsilon(\omega) = \varepsilon_1(\omega) + i\varepsilon_2(\omega)$  [19], which is mainly connected with the electronic structures. The real part  $\varepsilon_1(\omega)$  is derived from the imaginary part  $\varepsilon_2(\omega)$  by the Kramers-Kronig transformation. All the other optical constants, such as the absorption coefficient, reflectivity, and energy loss spectrum, are derived from  $\varepsilon_1(\omega)$  and  $\varepsilon_2(\omega)$ .

The calculated dielectric functions of pure and Ag-N-codoped (8,0) ZnO nanotubes are shown in Figure 5. The optical anisotropy are considered in this paper, and we have studied  $\varepsilon_2(\omega)$  under parallel polarization only, which is named as  $\varepsilon_2(\omega)^P$ . In Figure 5a, the pure (8,0) ZnO nanotubes have four peaks located at about 2.6, 8.3, 11.1, and 15.0 eV. The first peak located at 2.6 eV is mainly due to the transition from O 2p states to Zn 4s states. The second peak at 8.3 eV corresponds to transitions between the Zn 3d states and O 2p states. The peaks at 11.1 and 15.0 eV are associated with the electron transition between Zn 3d states and O 2s states. For the  $\text{Ag}_1$  configuration, the peak in the range from 5.0- to 13.0-eV energy region originates from the Zn 3d states to O 2p states and Zn 3d states to O 2s states. The peak in the low-energy region at about 0.1 eV mainly comes from the electronic interband transition between Ag 4d states and Zn 4s states in the

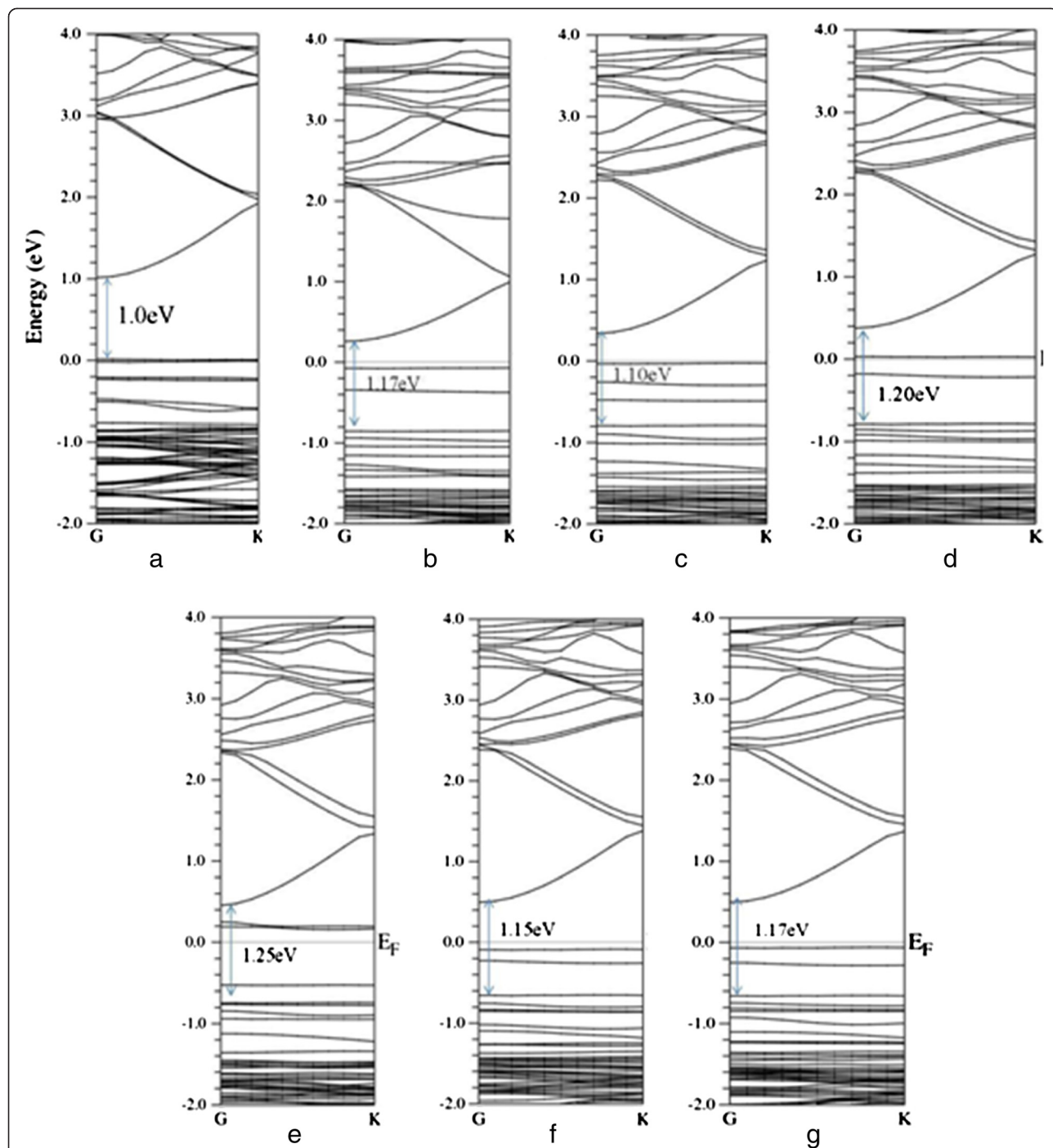


**Figure 3** Band structures of pure and Ag-N-codoped (8,0) ZnO nanotubes. (a) Pure (8,0) ZnO nanotube, (b)  $\text{Ag}_1$  configuration, (c)  $\text{Ag}_1\text{N}_2$  configuration, (d)  $\text{Ag}_1\text{N}_{3,4}$  configuration, (e)  $\text{Ag}_1\text{N}_{2,3,4}$  configuration, (f)  $\text{Ag}_1\text{N}_5$  configuration, and (g)  $\text{Ag}_1\text{N}_6$  configuration.

conduction band. The peak positions of the  $\text{Ag}_1\text{N}_2$ ,  $\text{Ag}_1\text{N}_{2,3,4}$ , and  $\text{Ag}_1\text{N}_{3,4}$  configurations are similar to that of  $\text{Ag}_1$  configuration except that the peaks are more intense because of higher N concentration. The peak at about 2.0 eV originates from the electronic transition from Ag 4d states to Zn 4s states for  $\text{Ag}_1$  configuration while it

originates from the electronic transition from Ag 4d to N 2p for  $\text{Ag}_1\text{N}_2$ ,  $\text{Ag}_1\text{N}_{2,3,4}$ ,  $\text{Ag}_1\text{N}_{3,4}$ ,  $\text{Ag}_1\text{N}_5$ , and  $\text{Ag}_1\text{N}_6$  configurations. A red shift occurred for the peak at about 0.5-2.0-eV energy region for the  $\text{Ag}_1\text{N}_2$ ,  $\text{Ag}_1\text{N}_{2,3,4}$ , and  $\text{Ag}_1\text{N}_{3,4}$  configurations with the increase of N concentration, because the electron transition energy from the

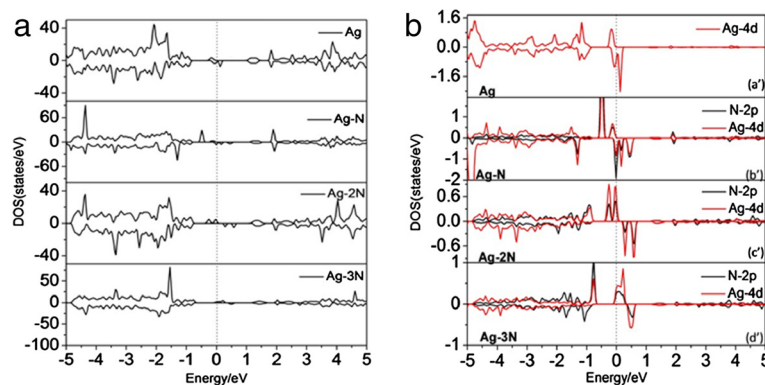


**Figure 4** Total DOS (a) and PDOS (b) of  $\text{Ag}_1$ ,  $\text{Ag}_1\text{N}_2$ ,  $\text{Ag}_1\text{N}_{3,4}$ , and  $\text{Ag}_1\text{N}_{2,3,4}$  configurations.

occupied impurity states to CBM has a red shift, and the gap of the occupied impurity states to CBM are 0.395, 0.366, and 0.201 eV, respectively. Figure 5b shows the dielectric function spectra of  $\text{Ag}_1\text{N}_2$ ,  $\text{Ag}_1\text{N}_5$ , and  $\text{Ag}_1\text{N}_6$  configurations. In Figure 5b, the peak at 1.0- to 5.0-eV energy regions has a red shift, and the volume of the peak

increases with the increasing distance of Ag atom and N atom.

Figure 6 shows the reflectivity and absorption spectra of pure and Ag-N-codoped (8,0) ZnO nanotubes. For the reflectivity of the pure ZnO nanotube, four peaks (located at 2.5, 6.0, 8.0, and 11.6 eV, respectively) can be

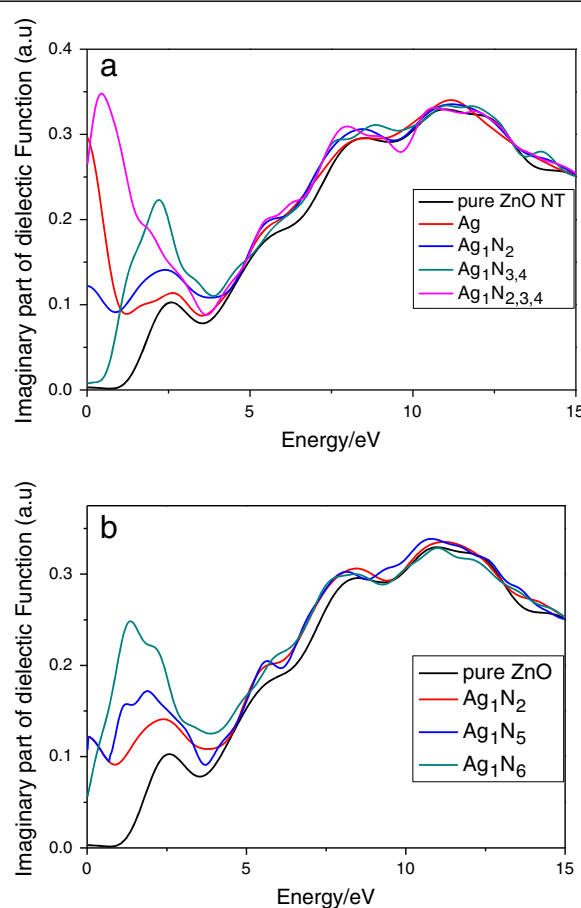


**Figure 5** Dielectric function spectra of pure and Ag-N-codoped (8,0) ZnO nanotubes. (a) Configurations of  $\text{Ag}_1$ ,  $\text{Ag}_1\text{N}_2$ ,  $\text{Ag}_1\text{N}_{2,3,4}$ , and  $\text{Ag}_1\text{N}_{3,4}$ . (b) Configurations of  $\text{Ag}_1\text{N}_2$ ,  $\text{Ag}_1\text{N}_5$ , and  $\text{Ag}_1\text{N}_6$ .

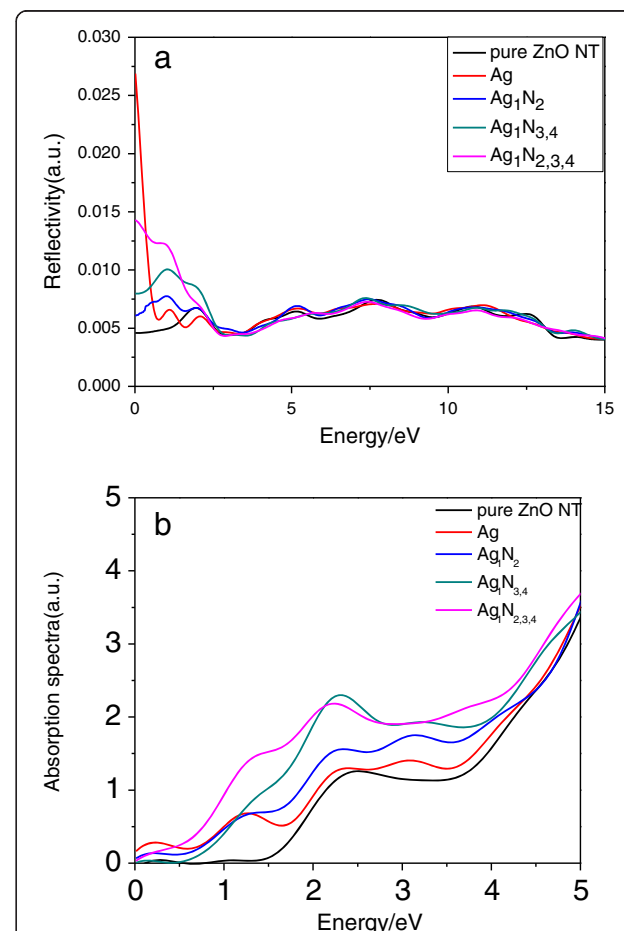


**Figure 6** Reflectivity (a) and absorption spectra (b) of pure and Ag-N-codoped (8,0) ZnO nanotubes.

observed, which correspond to the ones at 2.6, 8.3, 11.1, and 15.0 eV in  $\varepsilon_2(\omega)$ , respectively. For the  $\text{Ag}_1$  configuration, there is a new transition peak near the Fermi energy levels because Ag is doped into the ZnO nanotube, and it is associated with the electron transition between Ag 4d states and O 2s states. However, the peak at about 2.0 eV (in the visible light region) emerges for the configurations of  $\text{Ag}_1\text{N}_2$ ,  $\text{Ag}_1\text{N}_{2,3,4}$ , and  $\text{Ag}_1\text{N}_{3,4}$ , which is due to the electronic transition from dopant Ag 4d states to N 2p states, and it increases with the increase of N concentration. The  $R(\omega)$  of the pristine and Ag-N-codoped ZnO nanotube becomes smaller compared to that of the pure ZnO crystal [20]. This indicates that the transmissivity of the ZnO nanotube gets better in the visible light range. The optical absorption calculation shows that the absorption spectra of the Ag-doped and Ag-N-codoped ZnO nanotube become larger than pure ZnO nanotube. The foreign doping atoms in the ZnO nanotube have shifted the absorption edge towards visible light. These results show that doped ZnO nanotube has better optical absorption ability than pure ZnO nanotube in the visible and UV light range.

## Conclusions

In summary, we have studied the structural, electronic, and optical properties of pure and Ag-N-codoped (8,0) ZnO nanotubes using DFT. The configurations with Zn atoms replaced by Ag atoms are p-type semiconductor materials. For the N-doped ZnO nanotube configurations, the bandgap increases with the N concentration. When N atom replaces the second ( $\text{Ag}_1\text{N}_5$ ) and third neighbor ( $\text{Ag}_1\text{N}_6$ ) sites for Ag atom, the bandgap has a slight difference with the N that replaced the nearest neighbor site ( $\text{Ag}_1\text{N}_2$ ). The calculated dielectric function and reflectivity show obvious peaks in the visible light region which are due to the electronic transition from doped Ag 4d states to the Zn 4s conduction band for the configuration with Ag atoms replacing Zn atoms ( $\text{Ag}_1$ ) and Ag 4d state to N 2p state transitions for the Ag-N-codoped configurations, respectively. The peaks at about 0.5- to 2.0-eV energy region for the dielectric function have a red shift with the increase of N concentration. For the reflectivity, the transmissivity of the ZnO nanotube gets better in the visible light range compared with bulk ZnO.

## Competing interests

The authors declare that they have no competing interests.

## Authors' contributions

P-JW and C-WZ conceived the idea and designed the calculated model. X-YF carried out the electronic structure calculations and data analysis. X-JX performed the analysis method of optical properties. All authors read and approved the final manuscript.

## Acknowledgements

This work was supported by the National Natural Science Foundation of China (grant nos. 61172028, 61076088, and 11274143), Natural Science Foundation of Shandong Province (grant no. ZR2010EL017), Doctor Foundation of University of Jinan (grant no. xbs1043), and Technological Development Program in Shandong Education Department (grant no. J10LA16).

Received: 30 May 2013 Accepted: 1 August 2013

Published: 27 August 2013

## References

- Iijima S, Ichihashi T: Single-shell carbon nanotubes of 1-nm diameter. *Nature* 1993, **363**:603–605.
- Balasubramanian C, Bellucci S, Castrucci P, De Crescenzi M, Bhoraskar SV: Scanning tunneling microscopy observation of coiled aluminum nitride nanotubes. *Chem Phys Lett* 2004, **383**:188–191.
- Zhao M, Xia Y, Zhang D, Mei L: Stability and electronic structure of AlN nanotubes. *Phys Rev B* 2003, **68**:235415.
- Lee SM, Lee YH, Hwang YG, Elsner J, Porezag D, Thomas F: Stability and electronic structure of GaN nanotubes from density-functional calculations. *Phys Rev B* 1999, **60**:7788–7791.
- Qian ZK, Hou SM, Zhang JX, Li R, Shen ZY, Zhao XY, Xue ZQ: Stability and electronic structure of single-walled InN nanotubes. *Physica E* 2005, **30**:81–85.
- Shen X, Allen PB, Muckerman JT, Davenport JW, Zheng JC: Wire versus tube: stability of small one dimensional ZnO nanostructures. *Nano Lett* 2007, **7**:2267–2271.
- Zhou Z, Li Y, Liu L, Chen Y, Zhang SB, Chen Z: Size- and surface-dependent stability, electronic properties, and potential as chemical sensors: computational studies on one-dimensional ZnO nanostructures. *J Phys Chem C* 2008, **112**:13926.
- Ozgür U, Alivov Ya I, Liu C, Teke A, Reschikov MA, Doan S, Avrutin V, Cho SJ, Morkoc HA: A comprehensive review of ZnO materials and devices. *J Appl Phys* 2005, **98**:041301.
- Kim KK, Kim HS, Hwang DK, Lim JH, Park SJ: Realization of p-type ZnO thin films via phosphorus doping and thermal activation of the dopant. *Appl Phys Lett* 2003, **83**:63–65.
- Ryu YR, Zhu S, Look DC, Wrobel JM, Jeong HM, White HW: Synthesis of p-type ZnO films. *J Cryst Growth* 2000, **216**:330–334.
- Park CH, Zhang SB, Wei SH: Origin of p-type doping difficulty in ZnO: the impurity perspective. *Phys Rev B* 2002, **66**:073202.
- Wardle MG, Goss JP, Briddon PR: Theory of Li in ZnO: a limitation for Li-based p-type doping. *Phys Rev B* 2005, **71**:155205.
- Yan YF, Al-Jassim MM, Wei SH: Doping of ZnO by group-IB elements. *Appl Phys Lett* 2006, **89**:181912.
- Bian JM, Li XM, Gao XD, Yu WD: Deposition and electrical properties of N-In codoped p-type ZnO films by ultrasonic spray pyrolysis. *Appl Phys Lett* 2004, **84**:541–543.
- Ahn KS, Yan YF, Shet S, Todd D: Enhanced photoelectrochemical responses of ZnO films through Ga and N codoping. *Appl Phys Lett* 2007, **91**:231909.
- Wu MH, Pei Y, Zeng XC: Planar tetracoordinate carbon strips in edge decorated graphene nanoribbon. *J Am Chem Soc* 2010, **132**:5554–5555.
- Li YL, Zhao X, Fan WL: Structural, electronic, and optical properties of Ag-doped ZnO nanowires: first principles study. *J Phys Chem C* 2011, **115**:3552–3557.
- Usuda M, Hamada N, Kotani T, Van Schilfgaarde M: All-electron GW calculation based on the LAPW method: application to wurtzite ZnO. *Phys Rev B* 2002, **66**:125101.
- Zhang YG, Zhang GB, Wang YX: First-principles study of the electronic structure and optical properties of Ce-doped ZnO. *J Appl Phys* 2011, **109**:063510.
- Xie FW, Yang P, Li P, Zhang LQ: First-principle study of optical properties of (N, Ga) codoped ZnO. *Opt Commun* 2012, **285**:2660–2664.

doi:10.1186/1556-276X-8-365

Cite this article as: Feng et al.: Electronic structures and optical properties for Ag-N-codoped ZnO nanotubes. *Nanoscale Research Letters* 2013 **8**:365.